

Electron tunneling into single crystals of $\text{YBa}_2\text{Cu}_3\text{O}_{7-\delta}$

J. M. Valles, Jr.,* R. C. Dynes, A. M. Cucolo,[†] M. Gurvitch,[§] L. F. Schneemeyer, J. P. Garno, and J. V. Waszczak

AT&T Bell Laboratories, 600 Mountain Avenue, Murray Hill, New Jersey 07974

(Received 11 April 1991; revised manuscript received 1 July 1991)

We have fabricated tunnel junctions between chemically etched single crystals of $\text{YBa}_2\text{Cu}_3\text{O}_{7-\delta}$ and evaporated metal counterelectrodes that exhibit reproducible characteristics. Above the bulk critical temperature of $\text{YBa}_2\text{Cu}_3\text{O}_{7-\delta}$, T_c , the conductance as a function of voltage, $G(V)$, has a linear dependence on voltage and some asymmetry. Below T_c , additional structure associated with the superconducting state appears in $G(V)$. At $T \ll T_c$ there is a reproducible finite zero-bias conductance, which suggests that there are states at the Fermi energy in superconducting $\text{YBa}_2\text{Cu}_3\text{O}_{7-\delta}$. Junctions with Pb, Sn, Bi, Sb, PbBi, and Au counterelectrodes all show qualitatively similar behavior.

I. INTRODUCTION

Since the discovery of high-temperature superconductivity (HTSC), a wide variety of experimental techniques have been applied to the study of these compounds in an effort to understand the nature of the high- T_c superconducting and normal state. On the basis of past experience on conventional superconductors, electron-tunneling measurements on high-temperature superconductors have the potential to reveal a great deal about HTSC. Tunneling measurements probe the renormalized quasiparticle density of states in superconductors and hence can give a measurement of the energy gap and provide information about the pairing mechanism responsible for the superconducting state.¹

Tunneling measurements only probe the density of states within a region on the order of the superconducting coherence length ξ , which is extremely short in high-temperature superconductors. In orthorhombic $\text{YBa}_2\text{Cu}_3\text{O}_{7-\delta}$, the coherence length is anisotropic, with $\xi_c \approx 3-4$ Å in the direction normal to the Cu-O planes, and $\xi_{ab} \approx 15-25$ Å along the planes, as deduced from the extrapolated values of the upper critical fields.² Single crystals of $\text{YBa}_2\text{Cu}_3\text{O}_{7-\delta}$ are typically thin platelets oriented along the a - b planes; considering the extremely short ξ_c , tunneling into these platelets requires monolayer-level perfection at the surfaces. The surfaces of as-prepared single crystals which are subjected to long oxygen anneals so that they will superconduct do not satisfy this stringent requirement. We have overcome this problem by etching the surfaces of these crystals and making tunnel junctions on the freshly etched surfaces. With this method we have produced very stable junctions with reproducible characteristics.³

In this paper, we expand our previous discussion^{3,4} of the junction preparation method and the results obtained with these junctions. Section II contains a detailed discussion of the fabrication of the junctions and the measurement techniques. In Sec. III, we present our data and some arguments to support the assertion that the structure that we observe in the voltage dependence of

the tunnel junction conductance is related to the quasiparticle density of states of $\text{YBa}_2\text{Cu}_3\text{O}_{7-\delta}$. Since this structure only slightly resembles that of a BCS superconductor, we are faced with the problem of proving that the structure can be attributed to the quasiparticle density of states of the superconducting $\text{YBa}_2\text{Cu}_3\text{O}_{7-\delta}$ that is immediately adjacent to the tunnel junction. We dedicate a portion of this section to this issue. In Sec. IV, we discuss and compare our results to other experimental results on $\text{YBa}_2\text{Cu}_3\text{O}_{7-\delta}$. Section V contains a summary of our findings.

II. JUNCTION PREPARATION AND EXPERIMENTAL DETAILS

To measure the superconducting density of states on $\text{YBa}_2\text{Cu}_3\text{O}_{7-\delta}$ using electron tunneling it is necessary to first create a surface for the junction that has bulklike properties over a depth on the order of a coherence length. Various methods have been used to do this including crystal cleaving,⁵ break junction techniques on crystals and films,^{6,7} and point-contact probes that break the surface of a crystal or film.⁸ Also, with the improved techniques of film growth of $\text{YBa}_2\text{Cu}_3\text{O}_{7-\delta}$, it has become possible to grow superconducting films with top surfaces which are insulating over an extremely short length scale. Planar junctions made on such films⁹ and films with *in situ* grown artificial barriers¹⁰ have shown a very large degree of reproducibility and stability. We have attacked the surface problem with yet another technique that involves removing the insulating surfaces of annealed crystals or films and making planer tunnel junctions. These junctions are very stable and able to survive a number of thermal cycles. The conductance as a function of voltage in these devices is highly reproducible from junction to junction.

The single crystals of $\text{YBa}_2\text{Cu}_3\text{O}_{7-\delta}$ were grown by the flux method¹¹ and were annealed in oxygen for more than 3 weeks. The junctions were fabricated in the following manner. First, the crystals were etched either in 10 mM HClO_4 and 1 M NaClO_4 in water¹² for 5–30 min (etch

rate of $1000 \pm 100 \text{ \AA}/\text{min}$ or 1.0% Br (by volume) in methanol¹³ for 30–120 min (etch rate of $50 \pm 20 \text{ \AA}/\text{min}$). The surface of an etched crystal is dotted with crystallographically oriented square etch pits that are typically $20 \mu\text{m}$ on a side and $\approx 0.2 \mu\text{m}$ deep. Thus, a large number of a - b plane terminations are created on surfaces that are nominally oriented in the c -axis direction. This may be of great benefit for tunneling studies, given the difference in ξ_{ab} and ξ_c .² The etched regions appear very clean and shiny when viewed in an optical microscope. Etched crystals were heated for 5–10 min at 100°C in air in order to aid the formation of the tunnel barrier. The junctions were completed by evaporating the counterelectrode through a shadow mask. Junction dimensions were about $0.1 \times 1.0 \text{ mm}^2$ and resistances were between 5 and 1000Ω .

The nature of the barriers in the tunnel junctions is unknown, but the formation of high-quality tunnel junctions directly on the surface of oxide superconductors is quite common.¹⁴ We have observed that the room-temperature resistance of the junctions increases with time of heat treatment and depends on the counterelectrode material, i.e., Pb produces greater resistances than Au.

Four terminal measurements of the differential resistance were performed using standard low-frequency ac lock-in techniques. These resistances were inverted to obtain the differential conductance, $G(V)$. The conductance of a normal-metal–superconductor tunnel junction is given by

$$G(V, T) = C \int_{-\infty}^{+\infty} N_{\text{SC}}(E) \frac{df(E+eV)}{dV} P(E) dE, \quad (1)$$

where C is a constant that depends on the density of states of the normal-metal counterelectrode and $f(E+eV)$ is a Fermi function. The tunneling probability, $P(E)$, is expected to depend on matrix elements and band structure and not on temperature. Thus, all of the temperature dependence of $G(V)$ will arise from the Fermi function and any temperature dependence to the quasiparticle density of states $N_{\text{SC}}(E)$. [In a BCS superconductor, for example, the temperature dependence of $N_{\text{SC}}(E)$ enters through the temperature dependence of the energy gap.] At $T=0$, Eq. (1) reduces to

$$G(V, T=0) = CP(eV)N_{\text{SC}}(eV) \quad (2)$$

because the derivative of the Fermi function is a δ function in the low-temperature limit. Thus, $G(V)$ of a normal-metal–insulator–superconductor tunnel junction is proportional to the renormalized quasiparticle density of states of the superconductor for $T \ll T_c$.

III. RESULTS

We present data that come from four $\text{YBa}_2\text{Cu}_3\text{O}_{7-\delta}/\text{Pb}$, one $\text{YBa}_2\text{Cu}_3\text{O}_{7-\delta}/\text{Bi}$, and one $\text{YBa}_2\text{Cu}_3\text{O}_{7-\delta}/\text{Au}$ junctions that are representative of the results we have obtained on many of the over 100 junctions that we have made. For all measurable junctions, the structure in $G(V)$ below T_c was similar for different counterelectrode materials. The sharpness and

amplitude of the predominant features did vary somewhat from junction to junction, but remained nonetheless quite reproducible in a large number of junctions.

In Fig. 1(a) we show $G(V)$ normalized to $G(100 \text{ mV})$ of a $\text{YBa}_2\text{Cu}_3\text{O}_{7-\delta}/\text{Pb}$ junction at temperatures both above and below $T_c = 90 \text{ K}$. We present the data normalized because the high-voltage conductance depends on temperature, decreasing by approximately 15% from 10 to 180 K. We believe that this temperature dependence is due to some barrier effect. Perhaps the barrier width decreases as T decreases.

Above T_c , the conductance depends linearly on voltage at high voltages with an asymmetry of about 10% in the positive and negative voltage slopes [see Fig. 1(a)]. If the conductance is parametrized by

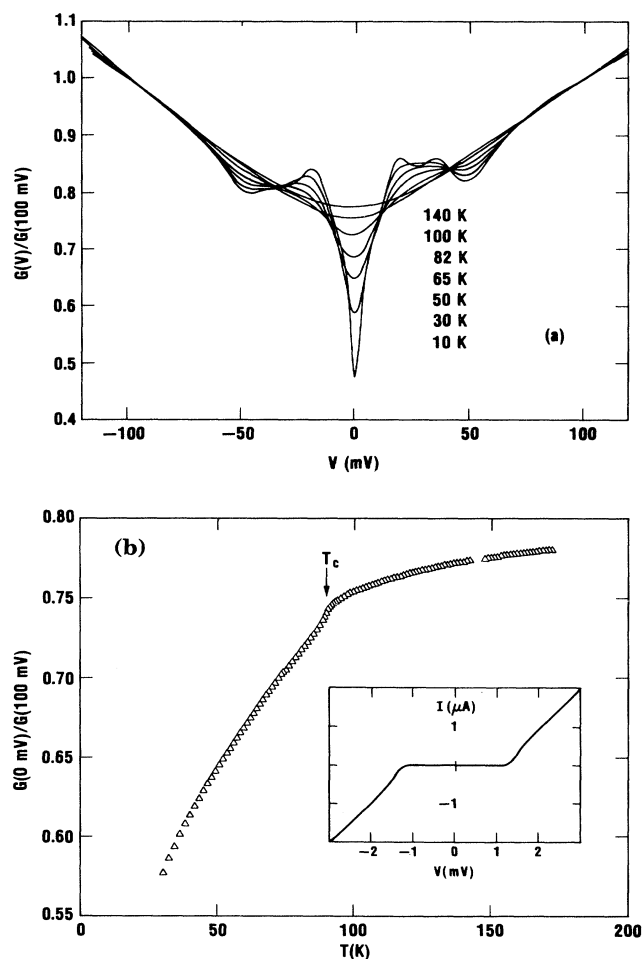


FIG. 1. (a) $G(V)/G(100 \text{ mV})$ for a $\text{YBa}_2\text{Cu}_3\text{O}_{7-\delta}/\text{Pb}$ junction, Sample 1, at the temperatures indicated. The lowest-temperature curve has the lowest zero-bias conductance. The polarity refers to the $\text{YBa}_2\text{Cu}_3\text{O}_{7-\delta}$ electrode. (b) Temperature dependence of $G(0 \text{ mV})/G(100 \text{ mV})$ of the junction. Inset: current vs voltage for a typical junction for $T < 1 \text{ K}$. Note the absence of leakage.

$$G(V) = G_0(\alpha|V| + 1), \quad (3)$$

where α is the slope for one of the polarities and G_0 is the extrapolated zero-bias conductance, then our data on many junctions show α to vary over about a factor of 2 from junction to junction. At voltages less than or equal to a few $k_B T/e$, the conductance is roughly parabolic as one would expect due to thermal effects. More quantitatively, we have calculated $\partial G/\partial V$ from data on junction 1 to show that the discontinuity in the slope predicted by the above is present. This is shown as the circles in Fig. 2(a) for $T=100$ K. From a smoothed version of $\partial G/\partial V$ [solid line in Fig. 2(a)] we can calculate $\partial^2 G/\partial V^2$ [see Fig. 2(b)] from which we can obtain the amount of thermal broadening in $G(V)$. The full width at half maximum (40 ± 4 meV) implies¹⁵ that the thermal broadening is $\simeq (4.8 \pm 0.5)k_B T$. This is *greater* than the amount of broadening that one would expect for a temperature-

independent density of states ($3.5k_B T$) and suggests that the density of states is temperature dependent (see later discussion).

Additional, finer structure that is somewhat asymmetric first appears in $G(V)$ at T_c . As shown in Fig. 3, the structure emerges at higher temperatures as broad bumps centered at approximately ± 25 mV and a strongly decreasing zero-bias conductance. These broad bumps develop finer structure and the zero-bias conductance continues to drop with decreasing temperature [see Fig. 1(a)].

These features first appear at T_c . In Fig. 1(b) we have plotted the temperature dependence of $G(V=0)/G(100$ mV) in order to demonstrate this. At T_c there is a discontinuity in $dG(V=0)/dT$ which is qualitatively similar, though much less pronounced, to what one would see due to the opening of an energy gap at T_c in a metal-insulator-BCS superconductor tunnel junction.

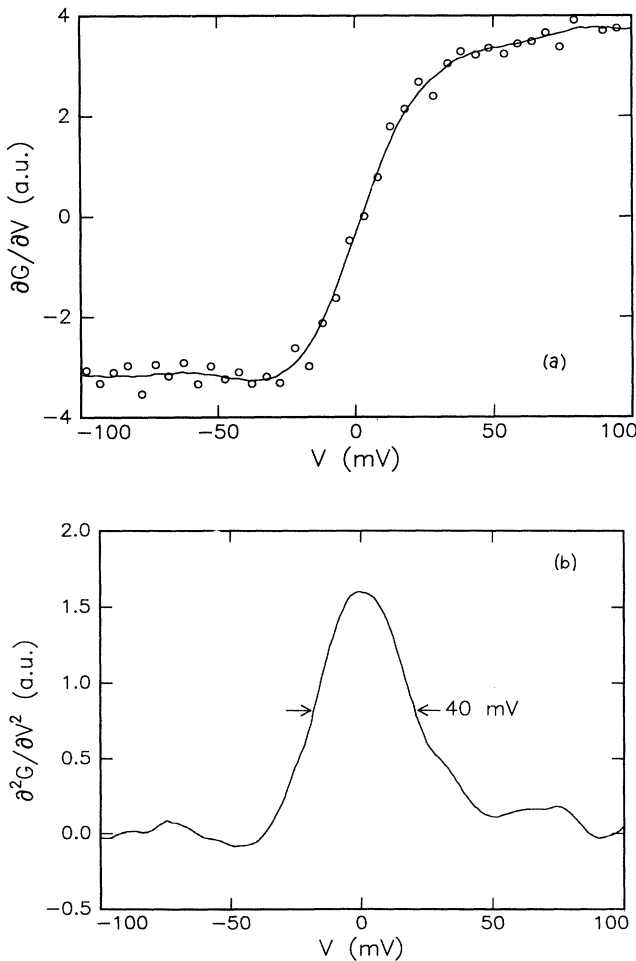


FIG. 2. (a) The circles are the numerically differentiated data and the curve is a smoothed version of these points. (b) $\partial^2 G/\partial V^2$ is calculated from the smooth $\partial G/\partial V$.

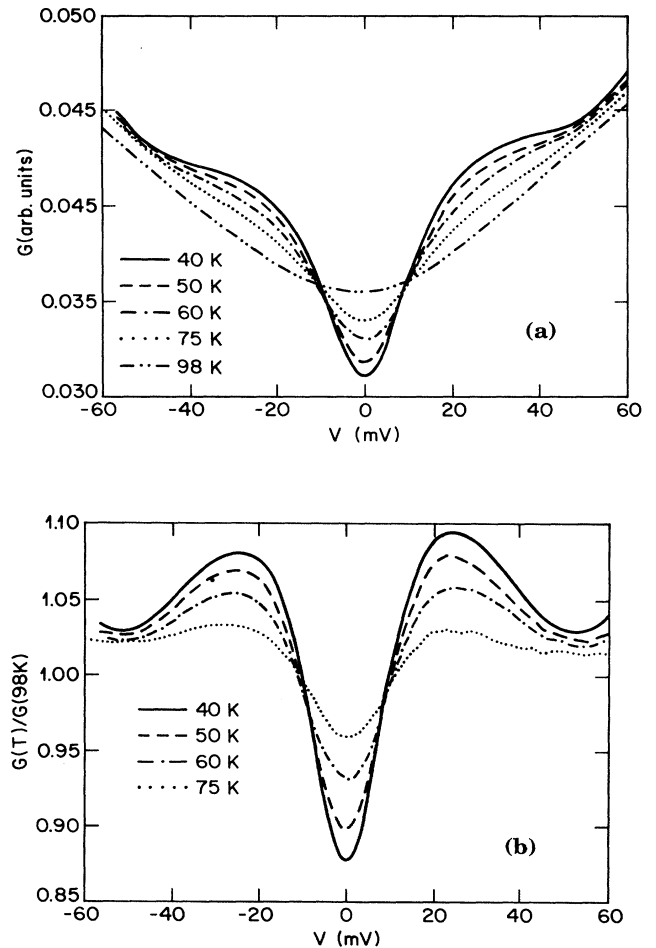


FIG. 3. Voltage dependence of the conductance at the temperatures indicated for a $\text{YBa}_2\text{Cu}_3\text{O}_{7-\delta}/\text{Pb}$ junction, Sample 2 different from that used for Fig. 1.

This is compelling evidence that the electrons are tunneling directly into *superconducting* $\text{YBa}_2\text{Cu}_3\text{O}_{7-\delta}$ —there is no thick (on the scale of ξ) reduced T_c layer at the surface. The weakness of the discontinuity compared to that expected for a conventional superconductor is consistent with the weakness of the structure in $G(V)$ at low temperatures compared to that of a conventional superconductor (see below).

It is useful to compare the data to the BCS form for the density of states:

$$N_S(E) = N_N(E) \frac{|E|}{(E^2 - \Delta^2)^{1/2}}, \quad (4)$$

where E is the quasiparticle energy measured relative to the Fermi energy, $N_N(E)$ is the normal-state density of states, and Δ is the energy gap. To accomplish this, we need to normalize the conductance in the superconducting state $G_S(V)$ to the conductance in the normal state, $G_N(V)$ at the same temperature. At low temperatures, this ratio will be proportional to $N_S(E)/N_N(E)$. Unfortunately, the upper critical magnetic field of $\text{YBa}_2\text{Cu}_3\text{O}_{7-\delta}$ is so high that we cannot measure $G_S(V)$ and $G_N(V)$ at the same temperatures. We thus choose to normalize by the $G_N(V)$ measured above T_c . In Fig. 4, we plot the data normalized in this way for various temperatures. After normalization, $G_S(V)$ more closely resembles a strongly coupled BCS density of states; more symmetric with a single dominant peak at positive and negative voltages. The dominant peaks move to higher voltages as the temperature is increased in a way that is qualitatively similar to that observed in tunnel junctions made with BCS superconductors. Also, the structure clearly starts to appear near T_c . Nevertheless, there remain substantial differences between these data and the BCS form.

We have performed a number of tests on our junctions to ascertain whether or not the behavior we see

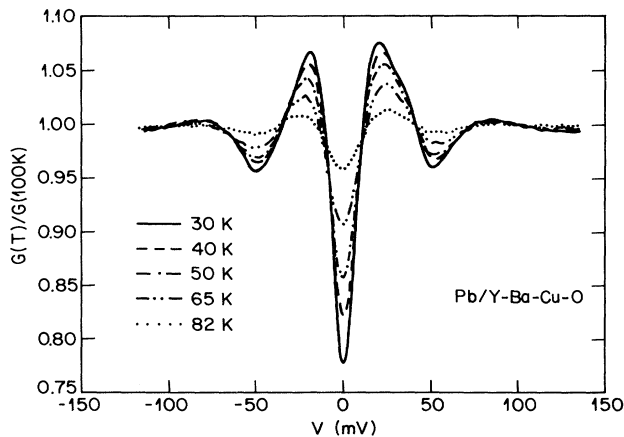


FIG. 4. Conductance as a function of voltage at different temperatures normalized by the conductance as a function of voltage at 100 K.

represents the intrinsic superconducting quasiparticle density of states in $\text{YBa}_2\text{Cu}_3\text{O}_{7-\delta}$. First, we assured ourselves that our tunnel junctions were of high quality. By using a Pb counterelectrode, we are able to determine if the conductance of the junctions is due to a single-step tunneling process. As indicated in the inset of Fig. 1(b), the junction conductance at voltages below the Pb energy gap (1.4 meV) is less than 1% of the conductance above the energy gap at temperatures $T \ll T_c(\text{Pb})$. This indicates that the only conductance process is tunneling.¹

Second, we show in Figs. 5(a) and 5(b) that the tunneling involves only single-step processes and no inelastic multiple-step processes. In Fig. 5(a), we show for $T \ll T_{c\text{Pb}}$ that there is fine structure in the junction con-

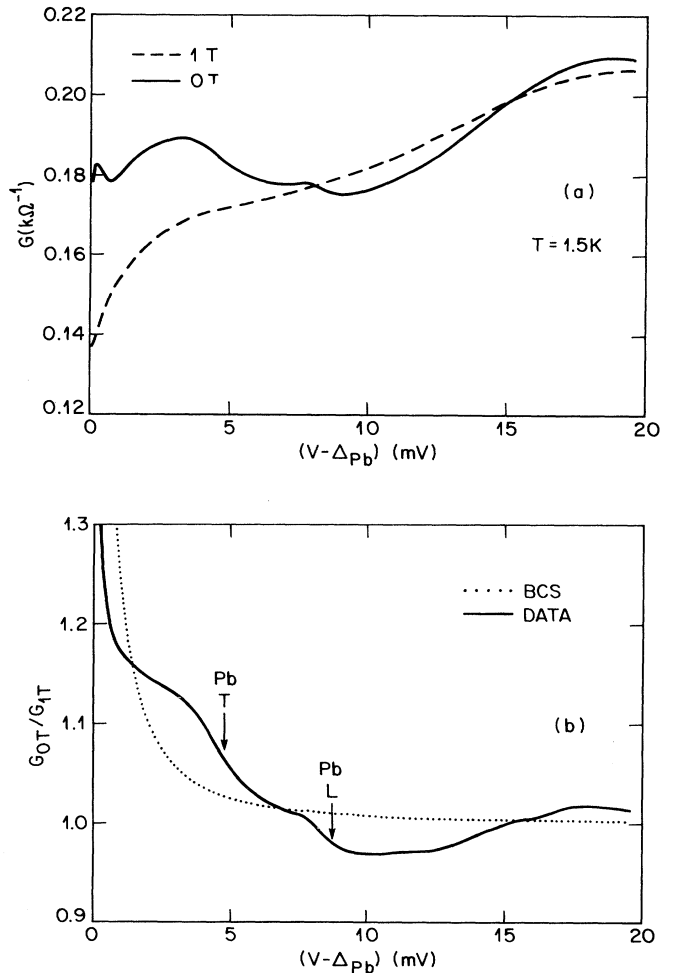


FIG. 5. (a) Conductance as a function of voltage measured relative to the Pb energy gap for Sample 1, a $\text{YBa}_2\text{Cu}_3\text{O}_{7-\delta}/\text{Pb}$ junction at $T = 1.5$ K in 0- and 1-T magnetic fields. The structure due to the Pb superconducting quasiparticle density of states is evident in zero field and is quenched in a 1-T field. (b) Conductance in 0 T normalized by the conductance in 1 T to bring out the structure due to the Pb quasiparticle density of states. The structures associated with the transverse (T) and longitudinal (L) phonons are indicated.

ductance in zero magnetic field that disappears in a field of 1 T. This structure is due to the phonon structure in the quasiparticle density of states of Pb. We demonstrate that this is so in Fig. 5(b), in which we plot the ratio of the conductance in zero field to the conductance at 1 T; a field which quenches the Pb superconductivity. The resulting normalized conductance shows features due to the longitudinal and transverse phonon peaks in Pb which are of the correct size and energy.¹⁶ If there were a multiple-step tunneling process or leakage conductance in this junction, then these features would be shifted, smeared, and reduced in amplitude.

Third, we have assured ourselves that the structure in $G(V)$ comes from a temperature-dependent density of states. In a superconductor, the gap structure and phonon structures in $N_S(E)$ are temperature dependent and disappear at T_c . To show that the structure that we observe in $G(V)$ results from a temperature-dependent density of states, we will first assume that it does not. This would imply that

$$G(V, T) = \int_{-\infty}^{+\infty} G(V', T=0) \frac{df(V+V')}{dV} dV', \quad (5)$$

so that a measurement of G at low temperatures would allow one to predict $G(V)$ at higher temperatures. It follows that deviations from this temperature dependence can be attributed to a temperature dependence of $N_S(E)$.

In Fig. 6, we show that there is a temperature dependence to $G(V)$ which we can attribute to a temperature dependence of the quasiparticle density of states of $\text{YBa}_2\text{Cu}_3\text{O}_{7-\delta}$. The dashed line gives the conductance at 90 K *calculated* using Eq. (5) with the conductance at 10 K serving as $G(V, T=0)$. The calculation contains more structure than and shows clear deviations from the measured 90-K conductance (solid line). From this comparison we conclude that the density of states that we are

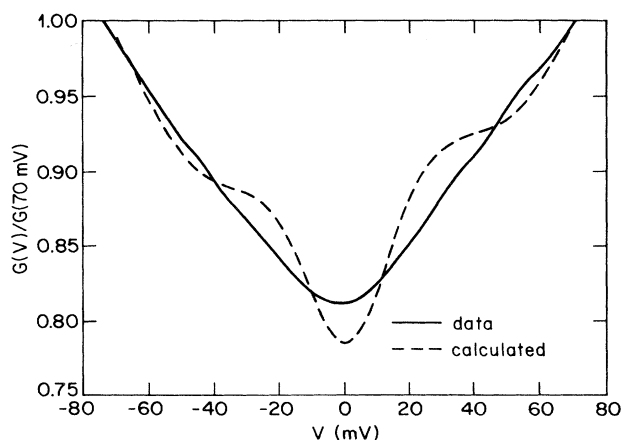


FIG. 6. The solid line is the measured conductance as a function of voltage at 90 K for a $\text{YBa}_2\text{Cu}_3\text{O}_{7-\delta}/\text{Pb}$ junction (Sample 1). The dashed line is the conductance calculated using the procedure described in the text. Note the structure in the calculated conductance as compared to the measured conductance.

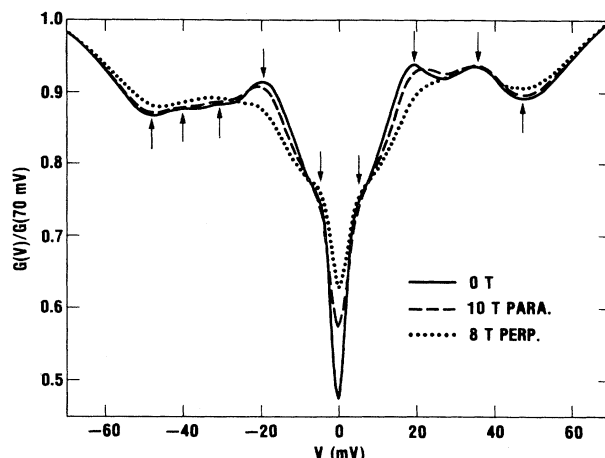


FIG. 7. Conductance as a function of voltage for a $\text{YBa}_2\text{Cu}_3\text{O}_{7-\delta}/\text{Pb}$ junction (Sample 1) in 0 T, 10.0 T parallel to the a - b planes, and 8.0 T perpendicular to the a - b planes. The arrows indicate features that are discussed in the text.

probing is temperature dependent as one would expect for a superconductor.

Having demonstrated that the conductance of these junctions is due to a single-step tunneling process and has a nontrivial temperature dependence, we can attribute the structure that we observe at low temperatures (under conditions for which Pb is not superconducting) to structure in the density of states of the $\text{YBa}_2\text{Cu}_3\text{O}_{7-\delta}$ material which is immediately adjacent to the tunnel barrier. We believe that this structure which develops at T_c is very closely related to the bulk intrinsic density of states of $\text{YBa}_2\text{Cu}_3\text{O}_{7-\delta}$, but we cannot prove this.

We emphasize this structure in Fig. 7 (solid line),

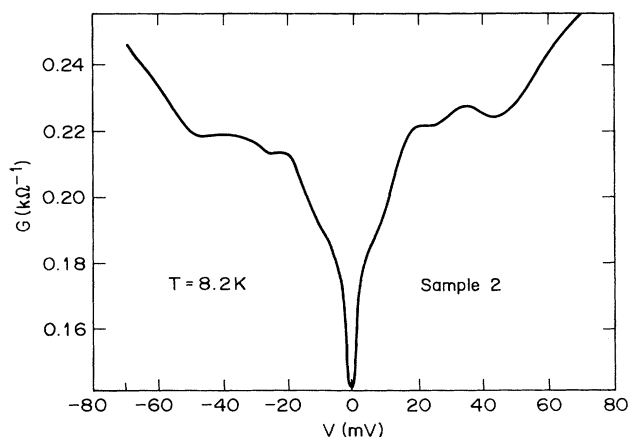


FIG. 8. Conductance as a function of voltage for a $\text{YBa}_2\text{Cu}_3\text{O}_{7-\delta}/\text{Pb}$ junction, Sample 2. Note that the two peaks at -31 and -41 mV in Sample 1 have merged into a single peak here.

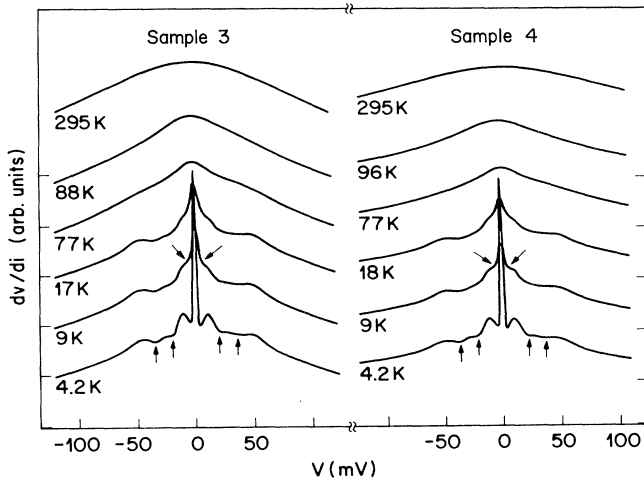


FIG. 9. Differential resistance as a function of voltage for various temperatures for two $\text{YBa}_2\text{Cu}_3\text{O}_{7-\delta}/\text{Pb}$ junctions, Samples 3 and 4. Note the similarities between the structures observed in these data and data from the other junctions.

where we have plotted $G(V)$ obtained at 10 K and in zero applied magnetic field over a finer voltage scale than in Fig. 1(a). Additional structure and the asymmetry in $G(V)$ are evident. The prominent features in $G(V)$ are peaks located at approximately ± 19 and $+36$ mV. There are two smaller broader peaks at approximately -31 and -41 mV. For some junctions, these features appear more as a single peak centered at -36 mV (see Fig. 8). Below about 25 K, features at ± 4 – 5 mV begin to emerge. The sharpness of these features varies a little from junction to junction but their positions are reproducible. We demonstrate this in Fig. 9, where we show the differential resistance of two other $\text{Pb}/\text{YBa}_2\text{Cu}_3\text{O}_{7-\delta}$

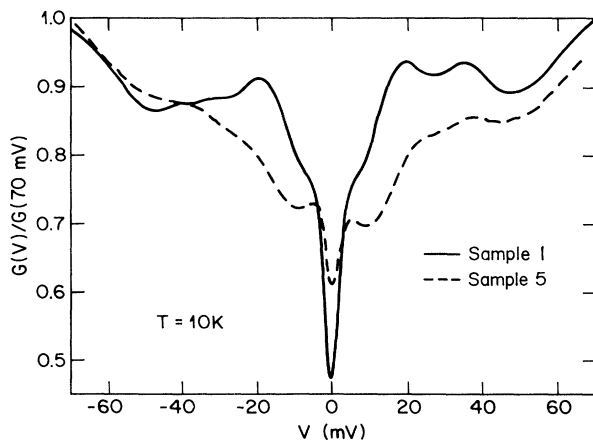


FIG. 10. Conductance as a function of voltage for two $\text{YBa}_2\text{Cu}_3\text{O}_{7-\delta}/\text{Pb}$ junctions. Note the peaklike structures at ~ 5 mV and the relatively weaker structure at higher energies in Sample 5 as compared to Sample 1.

junctions as a function of voltage at different temperatures. The same features are evident. For some of the $\text{Pb}/\text{YBa}_2\text{Cu}_3\text{O}_{7-\delta}$ junctions, such as Sample 5 in Fig. 10, the structures at ± 5 mV are stronger and appear as peaks in contrast to the data on Sample 1. The higher-energy features are evident in Sample 5, but they are weaker than in Sample 1. Figure 10 is an extreme example of the variation observed and most often the data appeared more like that of Fig. 7.

In addition to the features that we have described above, we have consistently measured a low-temperature zero-bias conductance, $G(0)$, on the order of 60–70% of the junction conductance at 0 mV at $T = T_c$. We know that this is not due to “leakage” because the ratio of the junction zero-bias conductance with Pb in the superconducting state ($T = 2$ K) to the junction zero-bias conductance with Pb in the normal state is much less than 1% [see inset of Fig. 1(b)].

The zero-bias conductance depends on temperature as shown for $10 < T < 90$ K in Fig. 11. It decreases with decreasing temperature much more slowly than one would expect for a BCS superconductor. To demonstrate how slowly $G(0)$ varies with temperature, we assume that $G(0)$ is zero at $T = 0$, and find that $G(0) \approx T^{0.18}$ as shown in Fig. 12. We have measured this temperature dependence to even lower T and shown that $G(0)$ in a magnetic field of ≈ 0.5 T continues to drop even at 0.1 K, a temperature 3 orders of magnitude below T_c .

Our measurements of $G(V)$ in applied magnetic fields give further evidence supporting the claim that most of the observed structure below T_c is related to the superconducting density of states of $\text{YBa}_2\text{Cu}_3\text{O}_{7-\delta}$. For a thin-film, type-II BCS superconductor, application of a magnetic field parallel to the plane of the film weakens the pairing interaction causing the transition temperature to drop and modifying the quasiparticle density of states. Specifically, the square-root cusp in the density of states becomes rounded and the spectral gap (which gives the

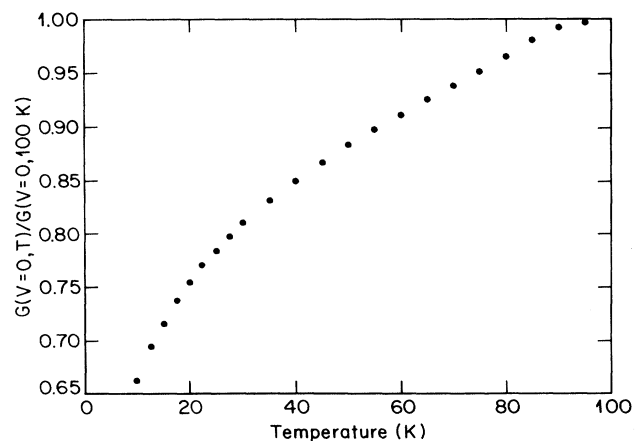


FIG. 11. Temperature dependence of the zero-bias conductance for a $\text{YBa}_2\text{Cu}_3\text{O}_{7-\delta}/\text{Pb}$ junction down to approximately 10 K.

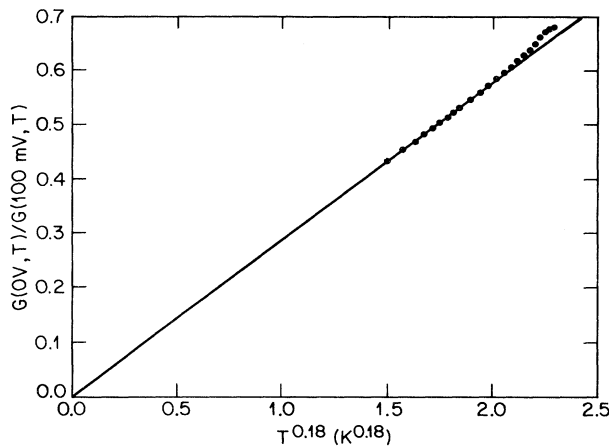


FIG. 12. Data from Fig. 10 plotted as a function of $T^{0.18}$ to demonstrate the extremely slow decrease of the zero-bias conductance as a function of temperature.

minimum energy required to create an excitation) decreases.¹⁷ These changes give rise to broadened peaks in $G(V)$ and an increased zero-bias conductance at finite temperatures.

Application of a perpendicular magnetic field gives rise to an inhomogeneous field distribution due to the penetration of vortices into the superconductor at the junction interface. Since the density of states in a vortex is approximately the normal-metal density of states,¹⁸ the presence of vortices will act to “dilute” the effect of the superconducting quasiparticle density of states on $G(V)$ in addition to modifying the density of states in the superconducting areas in the manner described above. Therefore, one expects the effects of a perpendicular field on $G(V)$ to be more dramatic than those of a parallel field.

In Fig. 7, we show the effect of a parallel magnetic field (dashed line) and a perpendicular magnetic field (dotted line) on $G(V)$. The features which appear to be most strongly affected by a parallel magnetic field are the zero-bias conductance, which increases, and the peaks at ± 19 and ± 5 mV, which broaden and shrink in a manner qualitatively similar to what we would expect for a BCS superconductor. Similar, but stronger, effects are observed for the perpendicular field case, as we might have expected based on the preceding discussion.

We also applied magnetic fields to junctions at higher temperatures and found the structure to be affected in the same qualitative way as the low-temperature data. This is shown in Fig. 13 where $G(V)$ of a $\text{YBa}_2\text{Cu}_3\text{O}_{7-\delta}/\text{Pb}$ junction at 60 K normalized by $G(V)$ at 95 K in 0 and 5 T are plotted. Again, the zero-bias conductance increases and the peaks diminish. This indicates that superconductivity is still evident at 60 K in the tunneling density of states.

We have also investigated the possibility that the observed structure in $G(V)$ reflects the properties of a

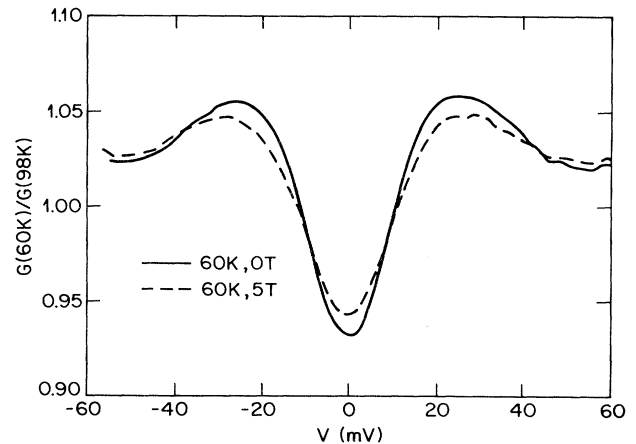


FIG. 13. Conductance as function of voltage for a $\text{YBa}_2\text{Cu}_3\text{O}_{7-\delta}/\text{Pb}$ junction at 60 K for 0- and 5-T magnetic fields applied perpendicular to the a - b planes.

$\text{YBa}_2\text{Cu}_3\text{O}_{7-\delta}/\text{Pb}$ interface rather than the intrinsic properties of the $\text{YBa}_2\text{Cu}_3\text{O}_{7-\delta}$ surface. If the former were true, then changes of the counterelectrode material would be expected to give changes in the structure of $G(V)$. To demonstrate that this is not the case, we have plotted $G(V)$ for Au and Bi counterelectrode junctions at 4.2 K in Figs. 14 and 15, respectively. While there are some subtle differences between these data and the $\text{YBa}_2\text{Cu}_3\text{O}_{7-\delta}/\text{Pb}$ data, the overall structures are the same; peaks near 20 mV, shoulders near 5 mV, and a large zero-bias conductance. This is a strong indication that $G(V)$ is directly related to the quasiparticle density

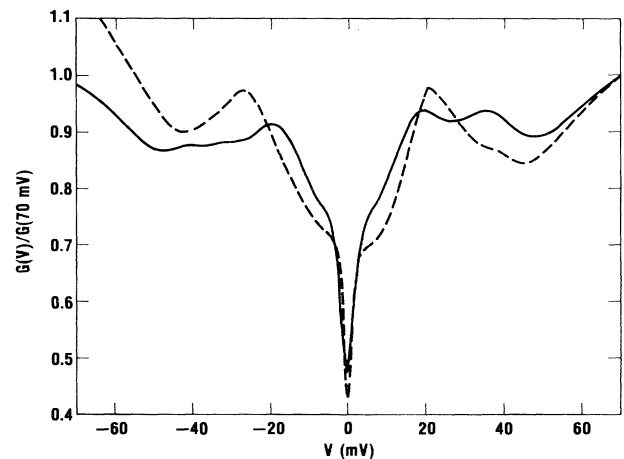


FIG. 14. Conductance as a function of voltage at approximately 10 K for a $\text{YBa}_2\text{Cu}_3\text{O}_{7-\delta}/\text{Au}$ (dashed line) and a $\text{YBa}_2\text{Cu}_3\text{O}_{7-\delta}/\text{Pb}$ junction (solid line).

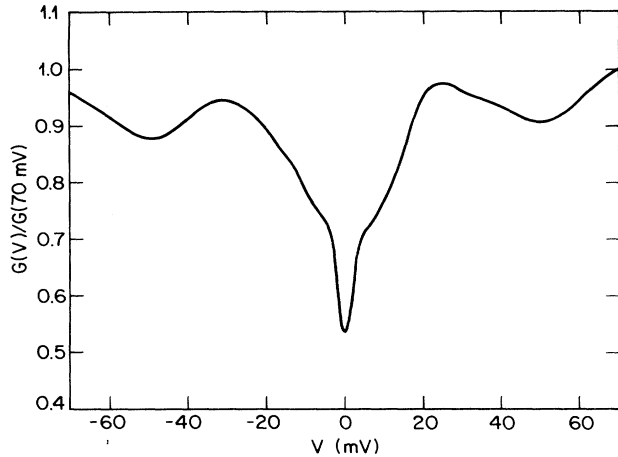


FIG. 15. Conductance as a function of voltage at approximately 10 K for a $\text{YBa}_2\text{Cu}_3\text{O}_{7-\delta}/\text{Bi}$ junction.

of states of the $\text{YBa}_2\text{Cu}_3\text{O}_{7-\delta}$. The small differences between $\text{YBa}_2\text{Cu}_3\text{O}_{7-\delta}/\text{Pb}$ and $\text{YBa}_2\text{Cu}_3\text{O}_{7-\delta}/\text{Bi,Au}$ conductances may find their roots in tunnel barrier shape and size effects.

As demonstrated by the data we have presented thus far on many junctions, and additional data not presented here, the observed structure in $G(V)$ is very reproducible. In the present studies, we have varied junction preparation parameters rather extensively (etchants, etching time, counterelectrodes, etc.) and obtained similar results. It is this remarkable reproducibility which gives us additional confidence in the intrinsic nature of the data.

Further confidence in the intrinsic nature of our data on $\text{YBa}_2\text{Cu}_3\text{O}_{7-\delta}$ comes from a comparison with other tunneling studies using different junction preparation techniques carried out by other groups. Results similar to ours have been obtained by Geerk and co-workers,⁹ and by Kwo *et al.*¹⁰ on epitaxial films, by Fournel *et al.*⁵ on cleaved single crystals, and by Takeuchi¹⁹ on sintered pellets. All of these groups observed a large zero-bias conductance at low temperatures and structure at 4–5 meV. We associate the 19-mV structure that we see to the 20-mV structure seen by Takeuchi,¹⁹ 16-mV structure of Geerk,⁹ and 30-mV structure of Fournel.⁵ We have also obtained similar results on thin films using the same etching technique.²⁰

IV. DISCUSSION

Our tunneling measurements yield structure in the quasiparticle density of states that does not conform to that of a simple superconductor. The tunneling conductance in the normal state and in the “background” of the superconducting state is a linear rather than a constant function of voltage. The linearity is striking and may indicate that the normal-state quasiparticle density of states depends linearly on energy around the Fermi energy.

There are multiple features of roughly equal strength in the superconducting density of states as opposed to two symmetrically located sharp peaks. This structure could arise for several reasons, including possible gap anisotropy in this highly anisotropic material, or a proximity effect. In the anisotropy picture, we can associate the structures at 5 and 19 mV with energy gaps along the c axis and in the a - b plane, respectively. In a proximity effect picture, the 5- and 19-meV features correspond to the gaps of weakly and strongly superconducting layers of material. Finally, there is a finite zero-bias conductance that may indicate the existence of states “in the gap” in the superconducting state. These characteristics suggest interesting possibilities for the density of states in superconducting $\text{YBa}_2\text{Cu}_3\text{O}_{7-\delta}$.

We attribute the linear dependence^{4,21,22} of the normal-state tunneling conductance to a density of states that depends linearly on energy at high energies:

$$N(E) = N_0(\alpha|E| + 1),$$

where α at positive and negative energies usually differ by $\approx 10\%$ and N_0 is the density of states at the Fermi energy. This form for $N_0(E)$ predicts a discontinuity in its derivative at the Fermi energy which is similar to the singular behavior observed in the tunneling density of states in disordered systems. In those systems, near the metal-insulator transition Fermi-liquid theory breaks down and singular corrections to the tunneling density of states, $\delta N/N_0 \propto E^{1/2}$ in three dimensions and $\delta N/N_0 \propto \ln(E)$ in two dimensions, due to disorder-enhanced spatial correlations between quasiparticle states appear. By analogy, we suggest that the linear energy dependence of the density of states in this material stems from similar correlation effects and a breakdown of the simple Fermi-liquid description. The thermal broadening in excess of $3.5k_B T$ of the structure in $G(V)$ is consistent with this picture. Similar excess thermal broadening is observed in the $G(V)$ of tunnel junctions made with disordered materials. This arises from the temperature dependence of the correlation corrections to the density of states. Indeed, the breakdown of a Fermi-liquid description of the normal state in these materials was proposed early by Anderson and Zou.²² They suggest that the resonating-valence-bond (RVB) theory predicts that the tunneling density of states should have a linear energy dependence. Alternatively Varma *et al.*²³ have developed a phenomenological description of the properties of the high- T_c normal state based on a marginal Fermi-liquid theory and suggest that the linear energy dependence of $N(E)$ is a consequence of this approach.

Alternatives to the explanation that the linear voltage dependence of the tunneling conductance stems from a density of states effect have been proposed. First, it was suggested that the linear voltage dependence results from barrier size effects.²⁴ In support of this picture, a reasonable fit to tunneling data on $\text{La}_{2-x}\text{Sr}_x\text{CuO}_4$ was obtained using a low-asymmetric-shaped tunneling barrier. This barrier was so low, however, that a significant temperature dependence to the tunneling conductance should be present. We do not observe a strong temperature depen-

dence and so argue against this model as a source of the linear background. More recently, Kirtley and Scalapino¹⁵ suggested that the linear background is due to inelastic tunneling effects involving a broad band of spin-fluctuation excitations. This linear background has been observed in the normal-state conductance in other high- T_c compounds, $\text{La}_{2-x}\text{Sr}_x\text{CuO}_4$,^{24,25} $\text{BaPb}_{1-x}\text{Bi}_x\text{O}_3$,⁴ and, most recently, $\text{Ba}_{1-x}\text{K}_x\text{BiO}_3$.²⁶ While this spin-fluctuation argument could apply to the cuprates, it will not apply to the bismuthates in which quantitatively similar linear backgrounds are observed but no spin fluctuations are possible. An alternative coupling to, for example, charge-density waves would have to be invoked. In addition, this model implies that the conductance of the tunnel junction at high voltages ($eV > k_B T$) decreases as the temperature decreases; behavior which is the *opposite* to that which we observe (see discussion of Fig. 1). Hence, we argue that the “linear density of states” model gives a more likely explanation for the linear background.

Finally, we note that some work using scanning tunneling microscopy²⁷ and point-contact²⁸ tunneling into high- T_c superconductors show a background conductance that depends on junction resistance. For high resistances $G(V)$ increases with V and for low resistances $G(V)$ decreases with V . We believe that this behavior results from the high current densities that are used in these devices. The joule heating that occurs at the tunnel junction interface can drive regions of the high- T_c superconductor near the interface into the normal state. The resistance of this region adds in series with the junction resistance, thereby reducing the “observed” junction conductance. The size and, hence, resistance of this normal region will increase with increasing voltage and decreasing junction resistance. Thus, in lower resistance junctions in which the current densities are relatively high, the background conductance can decrease with increasing voltage. It is important to note that these inverted backgrounds should be temperature dependent; heating effects will be more severe at lower temperatures. We have observed an inverted background in one of our lowest resistance junctions when we cooled it down to dilution refrigerator temperatures.

In preliminary measurements below T_c , multiple gap-like structures in $G(V)$ have been observed in Tl-Ba-Ca-Cu-O,¹⁹ and Bi-Sr-Ca-Cu-O,²⁹ similar to those in $\text{YBa}_2\text{Cu}_3\text{O}_{7-\delta}$, suggesting that they are a general property of the cuprates. Keeping in mind that these systems are highly anisotropic, we suggest a possibility that the multiple structures arise from multiple energy gaps: one at 19 meV associated with the a - b planes and one at 4–5 meV associated with the c axis. Indeed, the nonplanar etched surfaces provide for tunneling in both directions, as was pointed out above. If this interpretation is correct, then we estimate the geometric mean $\Delta_m = (1/\sqrt{3})(2\Delta_{ab}^2 + \Delta_c^2)^{1/2}$ to be 15.7 meV which corresponds to a $2\Delta/k_B T_c$ ratio of approximately 4.1; a number which is closer to the weak-coupling limit of 3.5 than many other measurements.

A second possible physical explanation for the multiple “gaplike” structure was put forth by Takahashi and Ta-

chiki.³⁰ These authors suggest that the copper-oxide superconductors have layer structures with strongly and weakly superconducting layers. Because the coherence length is so short, this results in an internal proximity effect where the more weakly superconducting planes (or chains) are weakly coupled to the strongly superconducting planes. As a result of the coupling, multiple gaps appear. At the moment, we see no reason why their effect should not be operative and find this a rather appealing explanation.

The finite zero-bias conductance could be due to several things such as (a) the presence of states at the Fermi energy of superconducting $\text{YBa}_2\text{Cu}_3\text{O}_{7-\delta}$, (b) the presence of both superconducting and normal metallic phases within the junction area, (c) a normal-metal surface on $\text{YBa}_2\text{Cu}_3\text{O}_{7-\delta}$ which superconducts due to the proximity effect, or (d) states at E_F that are induced by spin-flip scattering. In support of (a), the theory of Takahashi and Tachiki also predicts states at E_F that result from the coupling between weakly and strongly superconducting layers. If (b) is correct, then the structure that we observe is representative of the quasiparticle density of states but it is “diluted” by conductance paths into the normal metal. In view of the reproducibility of this effect, we judge this explanation unlikely. The short coherence lengths in this material make choice (c) a more likely explanation for our observations. In short coherence length material, the order parameter and the quasiparticle density of states can vary over small distances ($\xi_c \approx 3 \text{ \AA}$). Imperfections in the first ξ_c of the surface could create distortions in the measured density of states. Proximity of the surface to good bulk regions would still give it a bulk transition temperature. Again, the reproducibility of tunneling data on $\text{YBa}_2\text{Cu}_3\text{O}_{7-\delta}$ argues against this possibility.

Finally, the cuprates are antiferromagnetic insulators and as such are prone to have defects that have free spins. If the presence of spin defects is an issue, then the observed states in the “gap” could be due to spin-flip scattering resulting in gaplessness: choice (d). In conventional superconductors, if the spin-flip scattering rate $\hbar\tau_{\text{SF}} \sim \Delta$, gaplessness occurs.¹⁷ Tunneling studies of conventional superconductors with dilute magnetic impurities show behavior which is qualitatively similar to that shown in Fig. 1. Depending on the strength of the electron local moment interaction, only one impurity in 10^2 is necessary for such effects.³¹ A small density of defects in the copper-oxide planes might give a resultant moment and subsequent magnetic scattering. A problem with this explanation is the apparent reproducibility of the tunneling results in thin-film and single-crystal samples. It is difficult to imagine all samples having approximately the same density of spin-flip scattering centers unless such defects are intrinsic. We believe that the reproducibility of the size of the zero-bias conductance between junctions prepared in many different ways and the observed onset of structure at the bulk T_c argue against this possibility.

Thus, the reproducibility of the relative size of the zero-bias conductance makes it difficult to imagine that it is not related to the density of states of superconducting

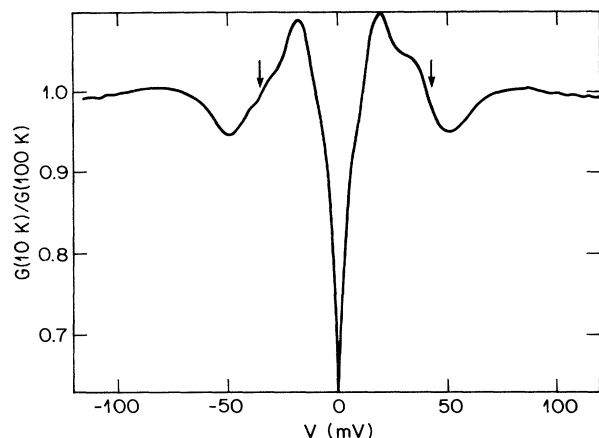


FIG. 16. Conductance data at 10 K from Fig. 1(a), Sample 1, normalized to the 100-K conductance. The arrows indicate the location of possible phonon structure in the quasiparticle density of states in $\text{YBa}_2\text{Cu}_3\text{O}_{7-\delta}$.

$\text{YBa}_2\text{Cu}_3\text{O}_{7-\delta}$. This result, taken at face value, certainly implies that there is a continuum of states below the gap. We tend to favor the explanation of Takahashi and Tachiki for the origin of these states.³⁰

Earlier we presented the conductance data in normalized form, pointing out that a single peak dominated the structure in $G_{\text{norm}}(V)$. The 36-meV peaks were transformed into shoulders by the normalization procedure. In Fig. 16, we plot $G_{\text{norm}}(V)$ at 10 K and note that these shoulders are reminiscent of the phonon structure in the quasiparticle density of states that one observes in a strongly coupled BCS superconductor. If this is the case and one assumes $\Delta \approx 19$ meV, then $V - \Delta = 23$ meV gives the energy of the phonon. Using the Allen-

Dynes-McMillan formula,³² $T_c = 0.15(\lambda\bar{\omega}^2)^{1/2}$, we find we need a $\lambda = 5$ for a $T_c = 90$ K. A McMillan-Rowell analysis¹ of the data gives $\lambda \approx 2$. These results suggest strong coupling. We note that the analysis of the linear resistivity suggests a small λ .³³ We also caution that this structure in the tunneling conductance is not strictly symmetric about zero bias. Eliashberg theory does not allow for any asymmetry in the normalized superconducting density of states and so a detailed analysis in these terms does not seem justified at the moment. Nevertheless, it is intriguing to speculate that perhaps this structure is a signature of the coupling mechanism and is of sufficient strength to account for $\lambda \approx 2$ — a strongly coupled superconductor.

In summary, we have reported tunneling measurements into single crystals of $\text{YBa}_2\text{Cu}_3\text{O}_{7-\delta}$. The reproducibility of these results gives us confidence that they reflect the intrinsic properties of $\text{YBa}_2\text{Cu}_3\text{O}_{7-\delta}$. At T_c , we see an abrupt change in the zero-bias conductance which shows that we are tunneling into the superconducting state. There are two gaplike features at 4–5 and 19 meV. This structure does not have a BCS shape and we consistently see a zero-bias conductance which is $\approx 60\%$ of the conductance at 100 mV, suggesting the possibility of states in the gap. There are several possible explanations for such states and we tend to favor that based on an internal-proximity-effect model.³⁰

ACKNOWLEDGMENTS

We thank, with pleasure, many colleagues for their suggestions and support. These include P. W. Anderson, J. M. Rowell, C. Varma, E. Abrahams, F. Sharifi, A. Pargellis, B. Batlogg, R. Cava, J. M. Phillips, T. Siegrist, and J. Geerk. J.M.V. acknowledges the support of the A. P. Sloan Foundation.

*Permanent address: University of Oregon, Eugene, OR 97403.

†Permanent address: Università di Salerno, 84100 Salerno, Italy.

§Permanent address: SUNY at Stony Brook, Stony Brook, NY 11794-3800.

¹W. L. McMillan and J. M. Rowell, in *Superconductivity*, edited by R. D. Parks (Marcel Dekker, New York, 1969), Vol. 1, p. 561.

²B. Batlogg *et al.*, *Physica* (Amsterdam) C **153-155**, 1062 (1988); Y. Matsuda *et al.*, *Solid State Commun.* **68**, 103 (1988).

³M. Gurvitch *et al.*, *Phys. Rev. Lett.* **63**, 1008 (1989); M. Gurvitch *et al.*, *Physica C* **162-164**, 1067 (1989); J. M. Valles, Jr., *et al.*, in *High-Temperature Superconductors; Fundamental Properties and Novel Materials Processing*, MRS Symposia Proceedings No. 169 (Materials Research Society, Pittsburgh, 1989).

⁴J. M. Valles, Jr. and R. C. Dynes, *Mater. Res. Soc. Bull.* **XV**, 44 (1990).

⁵A. Fournel *et al.*, *Europhys. Lett.* **6**, 653 (1988).

⁶J. Moreland *et al.*, *Phys. Rev. B* **35**, 8856 (1987).

⁷M. Lee, A. Kapitulnik, and M. R. Beasley, in *Mechanisms of*

High-Temperature Superconductivity, edited by H. Kamimura and A. Oshguyama, Springer Series in Materials Science Vol. 11 (Springer-Verlag, Heidelberg, 1989), p. 220; J. S. Tsai *et al.*, *ibid.*, p. 229.

⁸H. F. C. Hoevers *et al.*, *Physica* (Amsterdam) C **152**, 105 (1988); J. R. Kirtley *et al.*, *Phys. Rev. B* **35**, 8856 (1987).

⁹J. Geerk, X. X. Xi, and G. Linker, *Physica C* **162-164**, 837 (1989).

¹⁰J. Kwo, T. A. Fulton, M. Hong, and P. L. Gammel, *Appl. Phys. Lett.* **56**, 788 (1990).

¹¹L. F. Schneemeyer *et al.*, *Nature* (London) **238**, 601 (1987).

¹²B. Miller (private communication); J. M. Rosamilia *et al.*, *J. Electrochem. Soc.* **134**, 1863 (1987).

¹³R. P. Vasquez, B. D. Hunt, and M. C. Foote, *Appl. Phys. Lett.* **53**, 2692 (1988).

¹⁴B. Batlogg *et al.*, in *Proceedings of the International Conference on d and f band Superconductors*, edited by W. Buckel and W. Werber (Kernforschungszentrum Karlsruhe, Karlsruhe, 1982), pp. 401–403.

¹⁵J. R. Kirtley and D. J. Scalapino, *Phys. Rev. Lett.* **65**, 798 (1990).

¹⁶See, for example, D. J. Scalapino, in *Superconductivity*, edited

- by R. D. Parks (Marcel Dekker, New York, 1969), Vol. 1, p. 449.
- ¹⁷K. Maki, in *Superconductivity*, edited by R. D. Parks (Marcel Dekker, New York, 1969), Vol. 2, p. 1035.
- ¹⁸P. G. DeGennes, *Superconductivity of Metals and Alloys* (Addison-Wesley, New York, 1989).
- ¹⁹I. Takeuchi *et al.*, *Physica (Amsterdam)*, C **158**, 83 (1989).
- ²⁰A. M. Cucolo *et al.*, *Physica C* **161**, 351 (1989).
- ²¹R. C. Dynes (unpublished).
- ²²P. W. Anderson and Z. Zou, *Phys. Rev. Lett.* **60**, 132 (1988).
- ²³C. M. Varma, P. B. Littlewood, S. Schmitt-Rink, E. Abrahams, and A. E. Ruckenstein, *Phys. Rev. Lett.* **63**, 1996 (1989).
- ²⁴J. R. Kirtley, *Int. J. Mod. Phys. B* **4**, 201 (1990).
- ²⁵R. C. Dynes (unpublished).
- ²⁶J. F. Zasadzinski *et al.*, *IEEE Magnet.*, **27**, 833 (1991); F. Sharifi, A. Pargellis, and R. C. Dynes, *Phys. Rev. Lett.* **67**, 509 (1991).
- ²⁷T. Hasegawa *et al.*, *Jpn. J. Appl. Phys.* **30**, L276 (1991).
- ²⁸Q. Huang *et al.*, *Phys. Rev. B* **40**, 9366 (1989).
- ²⁹R. C. Dynes (unpublished).
- ³⁰S. Takahashi and M. Tachiki, *Physica B* **165-166**, 1067 (1990).
- ³¹A. S. Edelstein, *Phys. Rev.* **180**, 505 (1968).
- ³²P. B. Allen and R. C. Dynes, *Phys. Rev. B* **11**, 1895 (1975).
- ³³M. Gurvitch and A. T. Fiory, *Phys. Rev. Lett.* **59**, 1337 (1987).